




Review

Towards a Sustainable Greenhouse: Review of Trends and Emerging Practices in Analysing Greenhouse Ventilation Requirements to Sustain Maximum Agricultural Yield

Mohammad Akrami ^{1,*} , Alaa H. Salah ² , Akbar A. Javadi ¹, Hassan E.S. Fath ³,
Matthew J. Hassanein ¹, Raziye Farmani ¹, Mahdieh Dibaj ¹ and Abdelazim Negm ⁴ 

¹ Department of Engineering, University of Exeter, Exeter EX4 4QF, UK; a.a.javadi@exeter.ac.uk (A.A.J.); matthew.hassanein@ntlworld.com (M.J.H.); R.Farmani@exeter.ac.uk (R.F.); md529@exeter.ac.uk (M.D.)

² City of Scientific Research and Technological Applications (SRTA), Alexandria 21934, Egypt; alaa.h.salah@gmail.com

³ Environmental Engineering Department, School of Energy Resources, Environment, Chemical and Petrochemical Engineering (EECE), Egypt-Japan University of Science and Technology (E-JUST), Alexandria 21934, Egypt; hassan.fath@ejust.edu.eg

⁴ Water and Water structures Engineering Department, Faculty of Engineering, Zagazig University, Zagazig 44519, Egypt; amnegm@zu.edu.eg or amnegm85@yahoo.com

* Correspondence: M.AKRAMI@EXETER.AC.UK

Received: 20 February 2020; Accepted: 28 March 2020; Published: 1 April 2020



Abstract: Cultivation in open fields mainly depends on the location and time of farming, which itself highly depends on the quality and quantity of water for irrigation, weather conditions and soil characteristics. Water resources are highly dependent on the limited freshwater resources from the groundwater system, or rainwater. Countries in MENA (the Middle East and North Africa) rely mostly on desalination technologies for agriculture, due to water scarcity. Therefore, greenhouse (GH) agriculture can be developed to succeed in dealing with the water scarcity and provide sufficient sources of agricultural products as a sustainable solution. These indoor agriculture facilities, which are enclosed by transparent covers, can produce different sources of fruits and vegetables, using a controlled amount of water. By reducing the exchange rate of air with the outside environment, which is known as the confinement effects, greenhouses generate a suitable environment for the plants to grow under transparent covers to trap the sunlight. This raises the inside temperature above the maximum threshold levels, especially within the warm season, due to the high solar radiation intensity, having an adverse influence on the microclimate conditions and consequently the crop growth. In order to sustain maximum agricultural yield, greenhouse ventilation is an important parameter in which its trends and emerging practices were reviewed in this study.

Keywords: greenhouse; sustainability; ventilation; agriculture; energy and water efficiency

1. Introduction

Climate change, increasing population and lack of resources have led the countries around the world to choose sustainable development solutions. Increasing water-use efficiency, tackling water scarcity and poverty among societies and providing food are some of the main issues for sustainable development in the United Nations' 2030 agenda [1]. In order to supply food for the growing population, sustainable agriculture is essential. Open field agriculture is highly reliant on the agronomy's time and location, weather conditions and the soil properties. Compared to the open-field

agriculture systems, greenhouse (GH) systems allow to growing the plants very effectively under controlled environmental conditions. GH systems were originally conceptualised by Romans [2]. In the 1970s, the energy crisis was the main reason for modern horticulture development [3]. Since then, several studies have been performed to increase the resilience of such structures by analysing their interior environmental conditions to increase crop quality and production. GHs have been shown to reduce the water irrigation requirements by up to 90% compared with open field agriculture. This is very important in areas that have very little available freshwater and infertile soil [4,5]. In order to increase the horticultural yield, the micro climate conditions generated inside GHs can also be controlled by analysing the temperature, air velocity and humidity for optimal conditions of plant growth [6]. This helps to compensate for the possible negative effects by applying sufficient shading, proper ventilation and/or greenhouse cooling [7]. It is important in the Middle East and North Africa (MENA) region, especially within the current climate change era [8], where water is very scarce [4,5], and high temperatures, high solar intensity, and low humidity mean open field agriculture is not economical [5]. On the other hand, water scarcity has caused competition for water and instabilities [9], especially in the MENA region [10,11]. Therefore, the countries in this region have invested heavily in desalination technologies, which have the potential to be coupled with GHs and solar power to produce a free-standing solar-powered GH using water produced from desalination technologies, such as a zero-liquid discharge (ZLD), membrane distillation (MD) or solar still (SS) [12]. Previously, both experimental and computational studies have been performed to research the effects of ventilation, humidity, and solar intensity, on the indoor environment quality of different built environments [13], including GHs [14–16]. CFD (computational fluid dynamics) has been used to replicate GH conditions and study the effect of ventilation arrangements, air velocities, and other parameters on the conditions inside the GH [15]. However, all these depend on the type, location and direction of greenhouse and also the technologies that allow automated monitoring of greenhouse crops [17]. Although the Information and Communication Technologies (ICT) in water management for agriculture have advanced in recent years [18], they are not yet available in low income countries.

Greenhouses can be divided into several types based on their shape, utility, construction and covering materials. There is no single type of greenhouse that can be considered the best. However, there are advantages of each type for selected applications. Distinct types of greenhouses are designed to satisfy the specific needs of the agricultural system. This paper reviews the literature dealing with GH climate control technologies that have been researched and applied for many years. These are divided into: (i) Shape and orientation selection; (ii) ventilation systems; and (iii) cooling systems.

2. Greenhouse Shape and Orientation Selection

The shape and orientation of the greenhouses are mainly selected based on the solar radiation requirements, either to decrease the rate of cooling in hot regions, or maximize the rate of absorbed solar energy in the cold environments. This mathematical model developed by Gupta and Chandra analysed various energy conservation measures in order to achieve different design features for an energy efficient greenhouse in Delhi, India [19]. The developed model showed that the shape of the greenhouse is a significant parameter which envisioned that the rate of required heating for a gothic arch shaped greenhouse would be less than the heating requirements for the gable and Quonset shapes by around 2.6 and 4.2%, respectively.

In terms of the greenhouse direction, Sethi [20] showed that the heating requirements for an east-west oriented gothic arch greenhouse were nearly 2% less than for a north-south oriented one. It also showed that up to 30% could be saved on heating costs when the north wall is insulated in the east-west oriented gothic arch greenhouse. Sethi's study also predicted that by insulating the north wall, using night curtains, and utilizing inflated double wall glazing for the southern wall, the needs for greenhouse heating could potentially be reduced by around 80% [20]. It also analysed the total transmitted solar radiation for the five main types of single span shapes of greenhouses, which are even-span, uneven-span, vinery, modified arch and Quonset type [20]. The computed

results showed that uneven span types of GH could potentially secure the maximum solar radiation energy, while the Quonset shape received the least amount of radiation for all months during the experiment year, at any latitude. While the east-west orientation showed superior performance, due to absorbing a higher amount of radiation in winter and less in summer, the results of this study mainly emphasized that the shape of the greenhouses was more important than their direction for increasing GH performance. The optimal orientation is hard to analyse, since different parameters have simultaneous effects. Gupta et al. [21], showed that 45° clock-wise orientation had the lowest radiation loss during winter and the maximum loss during summer and therefore, orientation has to be selected carefully. Çakır, and Şahin [22] showed that the elliptic type of greenhouse provides optimal solar availability among the five types of the investigated greenhouse; even-span, uneven-span, vinery, semicircular and elliptic, while the orientation to the south was selected as a preferable direction in El-Maghlany et al.'s study [23]. Çakır, and Şahin also showed that for the low latitude angles ($< 24^\circ$), the east-west orientation provides optimal conditions, similar to Stanciu et al. [24] who also found this orientation could save energy load in even-span shape greenhouses in Romania.

Mono-span GHs are the simplest form of GH studied in the literature [16,25–30]. Investigations have focused on the effects of wind direction, vent combinations, wind speeds and the interaction of the wind with the crop. However, there are many other types of GH that have been studied, such as Multi-span [29,31,32], Open-roof [33,34], Saw-tooth [35], Venlo [36], Parral [37], Canarian [38,39], and Tropical [40,41] GHs. A full review of the different GHs can be found in Bournet and Boulard [42].

3. Ventilation Systems

In order to maximize the crop quality and quantity in warm regions, different cooling systems are utilized to remove the extra heat from greenhouses. This has been one of the major research areas studied by various researchers in this field. The principles incorporated by basic cooling techniques are listed below.

3.1. Ventilation

Ventilation is required to allow air movement and to maintain the lowest possible temperature gradient between the outside and inside of the greenhouse. This can happen naturally by means of the airflow, due to the density differences of the hot air inside the GH and the cooler ambient air, or forced ventilation, in which additional mechanical systems are deployed to improve the airflow and extract the heat from the greenhouse. In order to analyse the rates of ventilation, several studies have investigated the ventilation rates and their locations. Experiments on GH ventilation are performed either using a scale model in a wind tunnel or in situ [42]. Sase et al. [27], Okushima et al. [43], Boulard et al. [26,44], Lee et al. [45], Bailey et al. [46], Kacira et al. [47], and Teitel et al. [48] all analysed scale models of GHs using wind tunnels. In another scale model developed by Montero et al. [49], GH was submerged in a flume tank filled with water. The advantage of scale models is that wind velocity can be easily controlled [42]. Experiments using in situ GHs are also available for a variety of GH types, which all use full-size GHs to analyse airflow patterns and temperature contours. These studies have been performed on many different types of GH. The articles that studied the effect of ventilation on real GHs can be found in Kittas et al. [50,51], Boulard et al. [52], Wang and Deltour [53,54], Demrati et al. [55], Molina-Aiz et al. [56], Perez Parra et al. [57], Katsouas et al. [58], Ould Khaoua et al. [59], Bournet et al. [60,61], Teitel et al. [48,62], Baeza et al. [37], Fatnassi et al. [63], and Majdoubi et al. [64]. Most experimental studies focused on the ventilation rate of the GH, which is the number of greenhouse volumes renewed per hour [42]. The most common method of analysing the ventilation rate is the tracer gas technique [50,57,65]. This involves injecting an external gas, such as N_2O into the GH, and then measuring the time taken for the gas to decay to a certain level. The full procedure is described in Baptista et al. [65]. A number of experimental studies have analysed the temperature and velocity contours in the GH through physical modelling. Using scale models, Sase et al. [27] and Kacira et al. [47] used hot-wire anemometers and thermocouples placed at points

of interest around a GH to measure the air velocity and temperature. Okushima et al. [43] and Lamrani et al. [25] used thin thermocouples, and Lee et al. [66] used particle image velocimetry (PIV) in addition to anemometers to analyse the airflow throughout the GH. Boulard et al. [26] used a similar technique, with laser sheets instead of PIV, to visualize the air velocity. A full explanation of the use of PIV is given in Lee et al. [45], who compared it to CFD models and found good accuracy in the results. When physical models of GHs are used, due to the size, it is more difficult to accurately measure velocities and temperatures without incurring a high cost. Heber et al. [67] developed a similar technique to that used in the scale models, using thermocouples to measure temperatures and a sonic anemometer to measure ventilation rates and air velocities, which were also measured using an omni-directional hot wire probe. This method was used and improved upon during various studies, as it could be used to detect very low wind speeds, with an error of ± 0.04 cm/s [42]. Boulard et al. [52] measured the velocities and heat flows at vents and extrapolated the data to estimate the air exchange rate, which could then be compared to the tracer gas method described above. Boulard et al. [68] used a similar technique to infer the temperature distribution inside the GH, while Boulard et al. [69] looked at the turbulence in the GH. Bartzanas et al. [70,71], Shilo et al. [72], and Teitel et al. [62] also used a 3D sonic anemometer to measure air velocities and temperatures in the GH, and successfully compared the results to the tracer gas and CFD techniques. Wang and Deltour [54] used 2D sonic anemometers to measure the same parameters as Shilo et al. [72], Teitel et al. [48], and Molina-Aiz et al. [56] used a hot ball anemometer and smoke tracing technique to measure the air velocities. Besides the experimental techniques to analyse the rates of ventilation, computational fluid dynamics was also utilized to find this rate based on the air velocity, interior temperature and humidity levels. The CFD methods largely use ANSYS Fluent or COMSOL to divide the geometry into small elements, and solve the equations for mass, momentum and energy in each element [42]. The software then runs iterations until the solutions converge [73,74]. Generally, the surrounding air and external boundary conditions are also included, to minimize the effect of the boundaries on the flow of air through the GH. As Norton et al. [14] suggest, recent studies without the outdoor environment have sometimes shown no resemblance to experimental data. This is especially the case where the buoyancy effect is the driving force. Modelling the external domain, however, requires a much larger computational power, as the size of the geometry should be up to three times the GH ridge height upstream, seven times the height downstream and five times the vertical height [61]. Some other studies also modelled the external conditions, especially around a greenhouse [16,75,76]. The majority of studies available using the standard $k-\epsilon$ model, as it is the most popular and most widely used turbulence model for fluid modelling [45,48,56,59–61,64,70,77]. However, Mistrotis et al. [16], and Norton and Sun [78] both showed that the standard $k-\epsilon$ model could give poor results in certain cases. Both the Re-Normalization Group (RNG) $k-\epsilon$ model and realizable $k-\epsilon$ model have been shown to give better results in certain circumstances, but not enough information is available to say for certain which model is more effective [42]. However, Rouboa and Montero [79] suggest that the RNG model is most effective when studying the microclimates in the GH. Also, Roy and Boulard [76] studied the three models mentioned above in the same GH setup and found that the standard $k-\epsilon$ model gave the best convergence, but poor results, and the RNG $k-\epsilon$ model gave the best mixing of vortices. On the other hand, Nebbali et al. [80] found that comparing the results of the humidity, temperature and air velocity between the three models and experimental data of the same GH showed that the standard $k-\epsilon$ model had the lowest number of errors and was the most accurate. It should also be mentioned that the vast majority of CFD studies use the Boussinesq assumption to model the buoyancy effect [14], which is especially important for low wind speeds, where the buoyancy effect dominates [29].

Mostly, the studies were performed based on two-dimensional analysis, and assumed that the wind direction was perpendicular to the ridge axis of the GH, as for a 3D GH with a long length compared to the ridge height, the perpendicular flow should cause a 2D flow to develop that is consistent along the ridge. The work done by Sase et al. [27] in a scale model experimental study was replicated using CFD by Okushima et al. [28] and Mistrotis et al. [29], which both models successfully

obtained similar flow patterns to those found during the experiment. However, not all studies show good replication of the experimental data, both in situ and using scale models. This is especially the case when the wind direction is not perpendicular to the ridge, as this affects the ventilation rate, contrary to what was believed until CFD tools improved, and more studies were conducted to analyse the effect of the wind direction [42]. Campen and Bot [77], Shyklar and Arbel [81], and Teitel et al. [48] have all shown that the wind direction can improve the ventilation rate. As a result, and due to the improving computational facilities available, more studies are using 3D models to perform analysis of the velocity patterns under different conditions. Most studies have been performed using steady-state analysis and suppressing unsteady sections of the flow. However, some studies showed that as the force of nature is not steady, thus, the quantitative solutions of steady-state analysis cannot be fully accurate [14], and therefore, analysed unsteady characteristics of airflow around greenhouses [82–84]. Some studies were mainly focused on replicating the solar radiation in the GH in order to accurately model the effect of the radiation on the airflow and temperature distribution in the GH, while most of the CFD studies simplify the radiation model by calculating or experimentally obtaining temperatures or heat fluxes at the GH walls, instead of setting fluxes or using models to replicate the radiation at the external boundaries [14]. However, models have been developed in CFD that can accurately estimate the radiation from the sun based on the time of day and latitude and longitude coordinates of the GH's location. Wang and Boulard [85] developed a simple model to calculate the radiation on the walls of the GH, using theoretical knowledge. The models that have been used explicitly in CFD methods are the P1 model and the Discrete Ordinate (DO) model, which both solve the Radiative Transfer Equation (RTE) and calculate the luminance of the sun [42]. The DO model is much more commonly used, as it allows the user to set the transparency of materials and requires less computational time. Crop-based models were also analysed in previous studies to simulate the effect of the crops in the model, usually as a porous medium that is used to determine pressure loss in the flow [86]. Some models also use the porous medium to attempt to model heat fluxes from the plants, based on the solar radiation intensity, as well as convective air exchanges, in each element that models the crop area [42,86]. Lee and Short [87] studied the effect of the crop, using the porous medium method, and found that it reduced the ventilation rate by 12% for the same GH. Boulard also found that the presence of crop in the simulation reduced the ventilation rate by 28% [88], and transpiration rate reductions of 30% [89] were observed in areas where the airflow was weaker. Fatnassi et al. [63] also studied the effect of crops on the ventilation rate, and found that it decreased with larger crops, or proportionally to the leaf density. However, the process of photosynthesis is well analysed experimentally, but has not been accurately modelled using CFD [42]. This can affect the air temperature, humidity and CO₂ content in the air, and must also be modelled for more accurate simulations.

Different experimental techniques were developed to measure the rate of air exchange for natural ventilation. One of these showed that the air exchange rate was mainly affected by wind speed and also the effective vents opening [88]. In terms of wind speed, when it reaches a certain value, the rate of efficiency is reduced, as shown by the fact that the turbulent types of flows do not exceed 45% of the total heat flux [52].

In terms of ventilation rate, the American Society of Agricultural Engineers [37] recommends 0.04 m³s^{−1} per unit of floor area in summer. In another approach, the natural rate of ventilation was predicted to be in the range of 0.36 kg·s^{−1} to 1.65 kg·s^{−1} [37] for its specific GH model. In order to analyse sufficient rate of ventilation, the optimum temperature and humidity ranges for different plants have to be analysed, and these were studied by Campiotti et al. [90]. Computational fluid mechanic (CFD) techniques are used instead of, or along with, the experimental approaches for mapping the air flows and analysing the microclimate conditions within the GH. Such models can help new designs in order to maximize the crop quality [42], such as colour, texture, size, flavour and nutraceutical value [91]. For example, the effects of sidewall vents on buoyancy-driven natural ventilation in parral-type GHs, with and without insect screens, were analysed using CFD [37], which resulted in a novel GH design

utilizing two ventilators on the opposite sidewalls combined with a roof ventilator and higher rate of air exchange and lower inside temperature.

Several studies worked on different systems to have forced ventilation. Fan cooling is one such mechanical system showing little advantage over natural ventilation [92]. Adding evaporative pad cooling to the fans increased the rates from $0.05 \text{ m}^3/\text{m}^2\cdot\text{s}$ to $0.13 \text{ m}^3/\text{m}^2\cdot\text{s}$, while the temperatures of both air and canopy also decreased [92]. The two main forces behind the ventilation of the GH are the 'stack effect' or 'buoyancy effect', which is caused by different temperatures that induce density gradients in the air, and the forced convection associated with air velocity, due to the wind [42]. Sase et al. [27] experimentally observed that the transitional period between the two forces occurred at a wind velocity of 1–2 m/s, depending on the vent configurations, with lower velocities producing ventilation dominated by the buoyancy effect, and higher velocities producing ventilation dominated by wind velocity.

3.2. Effect of Forces Driving Ventilation

The airflow patterns in closed (no vents) GHs have been studied by various authors. The driving force of the air in these studies is only, due to the buoyancy effect, as no external air can enter the GH, and thus, external wind speeds have no effect. Lamrani et al. [25] experimentally studied a closed mono-span GH with different wall conditions, and found that for symmetrical boundary conditions, two counter-rotative air loops formed when a floor heat flux was first applied, but this developed into a single loop under steady-state conditions. The temperature within the GH was found to decrease very rapidly at the first 5 cm above the floor, and then gradually decrease with increasing height. Montero et al. [31] and Bournet et al. [32] studied a closed multi-span GH under night-time conditions and found that two counter-rotative flows developed, due to the design of the GH.

The effect of the wind speed on the force in ventilated GHs has also been studied. Sase et al. [27] experimentally found that the air velocity increases, due to the effect of wind and stack by about 1–2 m/s. This has also been analysed by Mistrotis et al. [16], Kittas et al. [50], and Papadakis et al. [30], who all found the wind speeds above which the buoyancy effect can be neglected lie between 1.5 m/s and 2.0 m/s. Furthermore, Boulard and Baille [93] found that the actual value depended on the GH geometry and vent locations, and the temperature difference between the inside and outside of the GH.

Studies have been performed with low-velocity wind speeds, where the buoyancy effect still dominates. Boulard et al. [26] compared a scale model and CFD study of the same mono-span GH with a single vent. They found that with no external wind, the experimental and CFD results both showed that the air came through the vent and moved towards the floor, before creating a single loop of air circulation around the GH, with the highest air velocities found close to the walls, decreasing to very low velocities in the centre. The comparison between the two also showed very good agreement. The temperatures were also in good agreement, with a rapid decrease in temperature at the floor, remaining the same until the roof, where a further decrease occurred. Sase et al. [27] also experimentally studied a scale model mono-span GH with vents on the walls and at the centre of the roof, for low-velocity wind speeds, and found that the air entered through the side vents, was warmed by the floor, and then moved upwards and exited through the roof vents. The same GH was investigated by Okushima et al. [28] and Mistrotis et al. [29] using CFD. Okushima et al. [28] obtained similar results to the airflow pattern found by Sase et al. [27], although computational resources were limited at that time. Mistrotis et al. [29] also simulated the heat fluxes involved, and for both a zero-wind speed and a 0.2 m/s wind speed, quantitatively produced the same results as Sase et al. [27]. Mistrotis et al. [29] also studied a multi-span GH using CFD with various vent combinations, which showed that a combination of both roof and side vents was required for efficient ventilation when the method was via the buoyancy effect. They also proved that when the ventilation was buoyancy-driven, the solar radiation intensity had a significant effect on the ventilation rate, as higher temperatures produced larger gradients, which increased the buoyancy effect and raised the ventilation rate. Similarly, Baeza et al. [37] showed the effect of the vent combinations on a parallel

GH (Almeria type), validated by an experimental method, and proved the importance of side vents in increasing the ventilation rate when the ventilation was buoyancy-driven.

There have been many more studies that analyse the ventilation of the GH at high wind speeds, when the buoyancy effect has a negligible impact on the ventilation. The most common type of study is on a mono-span GH. Sase et al. [27] studied a mono-span GH at higher wind velocities, where the wind effect dominates the ventilation rate, and found that the airflow pattern and temperature distribution did not change with higher wind speeds. However, the temperature rise was found to decrease proportionally to the logarithm of the wind speed [27]. Okushima et al. [28] and Mistrotis et al. [16] both validated the findings using CFD. Bartzanas and Kittas [94], and Bartzanas et al. [70] used CFD to study the effect of different vent configurations on the ventilation rate of the GH, and concluded that using roof and side vents could double the ventilation rate when compared to only using side vents. They also concluded that the temperature difference between the inside and outside and the wind velocity at plant level should be considered to optimize ventilation, and that the height of the side vents greatly affected the airflow pattern. Montero et al. [49] performed an experimental study on a similar GH, which resulted in very similar airflows to those in Bartzanas and Kittas [94]. Boulard and Wang [89], and Boulard et al. [68] studied a mono-span GH, both experimentally and using CFD simulations with crops modelled, and found that the heterogeneity of the climate (the difference in temperatures in the GH) was affected by the strong airflow from the windward side to the leeward side of the GH, with strong temperature gradients also predicted at the floor. Boulard et al. [26] experimentally and computationally studied the air velocity and temperature in a mono-span GH with a single vent and two vents, when the wind direction was perpendicular to the GH ridge. They found that for the single-sided vent, the air entered the lower portion of the vent, formed a loop around the GH with fast-moving air at the walls and still air in the middle, and exited through the top of the vent. For the two-sided ventilation, the same loop developed, but the cool air entered the GH from both sides, causing lower temperatures.

Multi-span GHs have also been studied by some authors. Boulard et al. [52] experimentally studied a wind parallel to the main axis of a multi-span GH with side vents, and obtained good agreement between results for the comparison of different ventilation measurement techniques. Boulard et al. [68] also experimentally studied the same GH and found that the section of the GH further upwind was warmer than the downwind section. The same results were produced using CFD models by Mistrotis et al. [16], who found that for a wind speed of 2.0 m/s, the external air entered through the leeward end and exited the windward end of the GH. Lee and Short [95] used CFD to analyse the effect of vents, opening area and a number of spans on a multi-span GH with side and roof vents, for different wind speeds. They analysed different conditions when the wind was parallel to the GH ridge, and found that the side vent significantly contributed to the air renewal rate of the GH. They also concluded that when the side vent was located at the bottom of the wall, the temperatures were more homogeneous, and therefore, the ventilation rate was better, whereas, for a high side vent, over half of the air was lost through the first roof vent [95].

3.2.1. Effect of Wind Direction

The effect of the wind direction on the GH has also been analysed [96]. Teitel et al. [48] experimentally and computationally investigated a multi-span GH with different wind directions, and found that for wind directions that were not perpendicular to the vents, the general trend was that there was an inflow at the leeward part of the vent, and an outflow at the windward part. They also found that the lowest ventilation rate occurred when the wind direction was at an angle of 30° to the vents, and the highest ventilation rate when the wind direction was at an angle of 60°. However, the results of Shyklar and Arbel [81] disagreed, showing that the ventilation was most efficient with a wind direction perpendicular to the vent, and least efficient when the wind was parallel to the vent. Campen and Bot [77] also showed that small variations in the wind direction could increase ventilation rates by large amounts. Bartzanas et al. [97] achieved a similar air-flow pattern to Teitel et al. [48], finding that

the windward end of the GH was consistently warmer than the leeward end for a wind parallel to and at an angle of 45° to the GH ridge.

3.2.2. Effect of Greenhouse Dimensions

The ventilation rate and air-flow pattern are strongly affected by the length and type of the GH, particularly the number of spans. Mistrotis et al. found that the same GH design with continuous vents and a different length had different flow patterns, and Kacira et al. [98] and Molina-Aiz et al. [99] found that the ventilation rate of a GH decreased exponentially with an increasing number of spans, with the latter also showing an increase in temperature at the plant level. Lee et al. [45,66] found that increasing the number of spans led to different flow patterns, with a GH with more spans developing flows that move against the wind direction.

The height of the GH also appears to affect the ventilation, although very few studies of this have been reported. Boulard and Fatnassi [100] used CFD to study the ventilation of three GHs varying only in their height, and concluded that increasing the height of the GH decreased the temperature. However, this has not been experimentally studied, due to the difficulty and cost of manufacturing and studying many different GHs. This is also the case with other GH dimensions that could affect the ventilation process and its energy requirements [19,101,102].

3.2.3. Effect of Vent Configurations

The effect of different vent configurations on the ventilation process has been studied in more detail. Bartzanas et al. [70] showed that adding side openings can increase the ventilation rate by a factor of five. Kittas et al. [51] also showed that the type of vent used could affect the ventilation rate, as roll-up side vents produced a more efficient ventilation rate than pivoting side vents, which also obstructed the air-flow and changed the internal pattern. The vertical position of the side vent was shown to have less of an effect on the ventilation rate [60,61], although lower side vents provided better air quality and a more consistent temperature at the plant level [103]. It has also been shown that ventilation is more efficient when vents are windward, but this may subject the plants to damage and cause more heterogeneity in the climate at plant level [59]. Many studies have looked at the effect of the size of the vent, and good agreement has been reached that increasing the vent size increases the air velocity at plant level and lowers the difference between the internal and external temperatures [103–105].

3.2.4. Analysing Humidity Range

Comparatively, little research has been performed on the humidity around the GH, and the crop transpiration rate under different conditions. Some experimental and CFD studies have been performed, which demonstrated that the similarities between the air temperature and humidity depend on the ventilation rate, external air humidity and plant transpiration mechanisms [106–108]. Humidity control in a GH has also been studied using a fog cooling system, with successful results [109,110]. Pearcy et al. [111] theorized that it was possible to measure the transpiration rate and leaf conductance in plants using simple measurements. Boulard et al. [112] showed that it was possible to measure the internal GH air humidity and temperature, and the internal airspeed and leaf transpiration rate, to determine the microclimate around the leaf. Boulard and Wang [89] implemented a crop model into a CFD simulation to model the transpiration rate of the plants, which was also used by Bartzanas et al. [70], Fatnassi et al. [113], and Majdoubi et al. [64]. Fatnassi et al. [114] also developed a linear crop model to analyse the effect on the humidity and found good agreement with experimental results. Hagishima et al. [115] experimentally studied the effect of the plant density on the transpiration rate of the plants and concluded that the plant transpiration rate was affected by the density of the plants, as greater plant density decreased the transpiration rate per plant. Kichah et al. [116] also estimated the transpiration rate, both experimentally and using a CFD model, and found good accuracy for the analysis, with an accurate estimation of the transpiration rate throughout the day.

4. Cooling Systems

4.1. Evaporative Cooling Systems

In order to cool the greenhouses, various evaporative cooling systems were developed and utilized to enhance the performance inside greenhouses.

In order to analyse the efficiency of the fan-pad systems, two distinct models were developed with fan and pad evaporative cooling systems [117], with the results showing the greenhouse efficacy could be increased through the use of such systems. When opening the fan-pad cooling systems, the relative humidity changes along with the greenhouses, from the pad panels to the exhaust fans, shows uniformity, but the temperature changes were usually non-uniform [118], which has to be considered while employing such mechanical systems within the greenhouses. The employed system in this study reduced the GH temperature from 30–33 °C to the range of 20–27 °C, and increased the humidity rate of 30–47% to 50–68%, where the outside climate conditions were 32 °C and 25% humidity. This showed how effective this system is for improving the GH microclimate conditions.

Thermodynamic simulations were performed to analyse the rate of freshwater production and energy consumption for a seawater greenhouse utilizing the humidification-dehumidification framework [119]. The results of this study proved that the greenhouse dimensions had the greatest overall effect on the amount of produced water and the required energy. While the wide shallow greenhouse offered 125 m³ of freshwater per day, the narrow deep structure produced only 58 m³ of water per day and used around five times more energy. While the effects of dimensions cannot be easily implemented for different greenhouses, researchers investigated the GH's width to length ratio [120]. Davies [121] proposed a liquid-desiccant system for GH in Abu Dhabi and compared it with two systems, the first of which was a GH with simple fan ventilation, while the second case employed conventional evaporative cooling. The results proposed that the novel liquid-desiccant cooling system could potentially lower the maximum summer temperatures by around 15 °C compared to a GH cooled by simple fan ventilation which is 5 °C lower than similar conventional evaporative cooling systems, while to be self-sufficient in water, the minimum rate of condenser efficiency was evaluated based on the concept of seawater GH [122]. When utilizing the evaporative cooling technique, there was a limitation on the inside air relative humidity, since it is highly dependent on the ambient air dry-bulb temperature [123]. The researchers of the same study also concluded that for the cooling machines and deep seawater cooling methods, the capacity of cooling and the flow rates are mainly dependent on the inlet and outlet temperatures of the condenser.

Condenser configuration for the HDH seawater GH desalination was analysed by Kabeel and El-Said [124], which showed that passive condenser was superior in terms of efficiency than the pump-driven one [125]. This was also investigated in another study by Mahmoudi et al. [126] in which they developed a mathematical model for a new proposed passive condenser in order to enhance its performance. Three methods of condensation were rigorously analysed; a pump-driven condenser, a passive cooling system with a condenser submerged in a water basin, and an external passive condenser connected to a basin of water located on top of the cooling unit. This study showed that the passive condenser could produce more water than the existing pump-driven system.

In terms of influential parameters on the rate of water production, studies raised the importance of the inlet air relative humidity [127]. In addition, the results of a similar study proved that as the inlet water flow rate increases, so does the water production, and the differential temperature and floor temperature both decreased. Moreover, by increasing the air into the system, the water production and floor temperature decrease and the differential temperature increases, which means the water produced can be used for irrigation using solar energy controllers [128] to water an area of about 2333 m² to plant tomato, cucumber, pepper and lettuce. This technology of seawater greenhouse could potentially be used to reduce the crop water requirement by almost 67% when compared to open-field cultivation [129].

Since the greenhouse humidity affects the transpiration rate and sensible heat flux [108], the effects of greenhouse cooling using a high-pressure fog system on its microclimate and on eggplant (*Solanum melongena*) crop response in the coastal area of western Greece were studied [130]. This study showed that fog cooling could potentially reduce mean fruit temperature by about 3 °C and keep the greenhouse air temperature below 32 °C, while the maximum temperature without cooling could reach 40 °C. This fogging system can control the rate of vapour pressure deficit (VPD) to analyse its effects on the greenhouse environment and tomato plant growth in the winter [131]. This study found that the VPD was dramatically reduced by the fogging system from 1.4 to 0.8 kPa on average at midday during the entire winter season. Furthermore, mean tomato biomass and yield were increased by 17.3% and 12.3%, respectively.

Roof evaporative cooling is another technique that can be utilized for sustainable greenhouse cooling. The reduction of air and surface temperatures induced by evaporative cooling of the outer roof of the greenhouse were compared experimentally by wetting the top of the canopy and soil surfaces [132]. Without the cooling system, the temperature differential was raised by $0.015\text{ }^{\circ}\text{C}\cdot\text{W}^{-1}\cdot\text{m}^{-2}$, while by wetting the upper surface of the roof, or the soil surface, the solar air heating was reduced to 0.0067 and $0.0016\text{ }^{\circ}\text{C}\cdot\text{W}^{-1}\cdot\text{m}^{-2}$, respectively, which justified the effectiveness of this cooling method.

4.2. Shading and Reflection

In order to decrease or avoid the intense solar radiation in the hot regions, shading and reflection are two methods that have been widely used. Radiometric properties related to global and diffuse PAR (photo-synthetically active radiation) of seven types of shading nets were quantified, including nets with colours and shading rates that are frequently utilized in hot regions [133]. The results revealed that the radiometric properties rely on both net porosity and colour under clear sunny and cloudy conditions; however, net reflectance staunchly formed on the net colour, net transmittance and absorptance, mainly based on colour and porosity.

4.3. Greenhouse Integrated System

Integrated Solar Green House (ISGH), which integrates the water desalination system into a greenhouse roof, could supply the water demands for the plants' growth with around one-third of the efficiency for the tilted solar stills [134], while also being self-sufficient for irrigation water [135]. This was studied by a mathematical model based on a set of heat balance equations to quantify the freshwater production. The differences in seasonal crop yields between the greenhouses with desalination systems and conventional roofs in arid climates were also investigated by Chaibi and Jilar [136]. Marí et al. [137] studied the functioning of a solar still integrated into a greenhouse for Mediterranean climatic conditions in south-eastern Spain. In this study, 28 water basins were located at the top of a greenhouse, and the inner surface of the roof was used as a condensation surface. The study depicted that opposite to what happens in the traditional solar stills, distillation resulted after solar noon and during the night mainly because of the low absorption of solar irradiation when the solar still is integrated into a greenhouse.

One other system that can be used for greenhouse cooling is the Earth-Air heat exchanger. This technique was developed mainly to analyse the exogetic functionality of a solar photovoltaic (PV) system [138] operating a heat exchanger in an underground air tunnel, which might be reasonably used for greenhouse cooling in the Mediterranean and Aegean regions of Turkey.

By coupling an aquifer cavity flow with one heat exchanger, a thermal model was presented to be used for agricultural cooling [139]. The results showed that the temperature of the air and plant could be kept within the range of 6–7 K and 5–6 K below ambient, respectively for an extreme summer day, and also 7–8 K and 5–6 K above ambient, respectively for an extreme winter night. The humidity control practices with soil fortifications were also studied by Entezari et al. [140] for a sustainable air-water-harvesting (AWH) greenhouse management.

5. Discussion

GHs are used to (i) provide plants with proper conditions (temperature and relative humidity), (ii) protect them from high wind speeds, (iii) reduce plants' need for water, (iv) provide plants with suitable solar radiation (required for the photosynthesis process), and (v) protect plants from open field diseases. The climate becomes colder further away from the Equator, and there is insufficient solar radiation for plant growth. In these regions, the main GH purpose is to warm the plant region by the GH effect. In contrast, the closer we get to the Equator, an additional system is added to the GH to reduce its temperature.

In hot regions, ventilation, shading and/or cooling systems are required for GHs to provide plants with a suitable temperature. There are many parameters affecting ventilation performance, such as wind direction, GH dimensions, vent configurations, humidity range, type of crop and cultivation system.

In dry regions, evaporative cooling systems are required to reduce GH temperature and raise GH relative humidity. The benefits of these systems appear when there is a lack of clean irrigation water. The Fan-Pad system is the easiest and least expensive cooling system. In order to maximize the benefit of this system, a new version of the system was developed known as the Seawater GH (humidification and dehumidification system). In addition to cooling offered by this system, freshwater is condensed before leaving the GH. Also, there is another type known as a roof evaporative cooling system which is used to achieve a good distribution for humidity in a GH. Additionally, there is a different type for evaporative cooling systems known as a fog-mist system. This system is easier to control when the water is sprayed directly into the GH cavity. This system should use water with suitable salinity for plant growth. In hot and high solar radiation regions, shading and reflection are used to avoid high temperatures. This system is mostly used with ventilation systems in wet regions where evaporative cooling systems are not preferred, as they would raise humidity inside the GH cavity.

6. Conclusions

Many studies have been carried out on the most suitable shape and orientation of the GH to maximize or minimize the solar radiation availability towards a more sustainable built environment. East-West orientation is recommended in areas far from the Equator to maximize the solar radiation availability in the winter and warm the GH. East-West orientation is recommended in areas near the Equator to minimize the solar radiation availability in the summer and reduce the GH cooling load. The uneven-span shape greenhouse receives the maximum solar radiation, and the quonset shape receives the minimum solar radiation during each month of the year at all latitudes. Different cooling systems are utilized to remove the extra heat from greenhouses and increase the quality and quantity of the crops. The effects of forces driving ventilation, wind direction, GH dimensions, vent configurations, and the humidity range were the parameters researched in the published studies. Evaporative cooling systems were also developed and utilized to enhance the performance of the greenhouse cavities, while shading and reflection was another influential parameter on such systems. While cooling is a necessity for the warm regions or hot seasons, heating for the cold seasons can be supported by renewable energy technologies to have a sustainable greenhouse. Future works should include integrating sensors and live data from the GH, using the internet, to provide smart automated feedback.

Author Contributions: Writing—original draft preparation, M.A., A.H.S., M.J.H., M.D., Writing—review and editing, M.A., A.H.S., A.A.J., A.N., H.E.S.F., R.F., M.D. All authors have read and agreed to the published version of the manuscript.

Funding: This work was supported by the British Council (BC) of UK (No. 332435306) and Science and Technology Development Fund (STDF) of Egypt (No. 30771), through the project titled “A Novel Standalone Solar-Driven Agriculture Greenhouse-Desalination System: That Grows its Energy and Irrigation Water” via the Newton-Musharafa funding scheme.

Acknowledgments: The authors would like to appreciate the anonymous reviewers for their insightful comments and suggestions.

Conflicts of Interest: The authors declare no conflict of interest.

References

1. UN SDGs. Transforming Our World: The 2030 Agenda for Sustainable Development. Resolution Adopted by the UN General Assembly. 25 September 2015. Available online: <https://sustainabledevelopment.un.org/post2015/transformingourworld> (accessed on 15 March 2020).
2. Janick, J.; Paris, H.S.; Parrish, D.C. The cucurbits of mediterranean antiquity: Identification of taxa from ancient images and descriptions. *Ann. Bot.* **2007**, *100*, 1441–1457.
3. Montero, I.J.; Teitel, M.; Baeza, E.; Lopez, J.C.; Kacira, M. Greenhouse design and covering materials. *Good Agric. Pract. Greenh. Veg. Crops* **2013**, *35*. Available online: https://www.researchgate.net/profile/Silvana_Nicola/publication/263922177_Quality_of_Planting_Materials/links/00b7d53c529871a853000000/Quality-of-Planting-Materials.pdf#page=51 (accessed on 25 March 2020).
4. Fath, H.E.S. Desalination and Greenhouses. In *Unconventional Water Resources and Agriculture in Egypt, The Handbook of Environmental Chemistry*; Negm, A.M., Ed.; Springer: Cham, Switzerland, 2017; pp. 455–483.
5. Fath, H.E.S.; Akrami, M.; Negm, A.; Javadi, A.A.; Farmani, R.; Mallick, T. A Novel stand-alone solar-powered agriculture greenhouse-desalination system; increasing sustainability and efficiency of greenhouses 2019. In Proceedings of the IAPE Conference, Oxford, UK, 14–15 March 2019.
6. Abdullahi, K.; Salah, A.H.; Fath, H.E.S. Micro Climatic Analysis of Sustainable Agricultural Greenhouse with Built-In Roof Solar Stills. In Proceedings of the IAPE-Conference, Oxford, UK, 14–15 March 2019.
7. Kittas, C.; Katsoulas, N.; Bartzanas, T.; Bakker, J. Greenhouse climate control and energy use. In *Good Agricultural Practices for Greenhouse Vegetable Crops: Principles for Mediterranean Climate Areas*; FAO Plant Production and Protection Paper; ISHS/FAO/NCARE: Rome, Italy, 2013; pp. 63–95. Available online: <https://research.wur.nl/en/publications/greenhouse-climate-control-and-energy-use> (accessed on 25 March 2020).
8. Schewe, J.; Heinke, J.; Gerten, D.; Haddeland, I.; Arnell, N.W.; Clark, D.B.; Dankers, R.; Eisner, S.; Fekete, B.M.; Colón-González, F.J. Multimodel assessment of water scarcity under climate change. *Proc. Natl. Acad. Sci. USA* **2014**, *111*, 3245–3250. [[CrossRef](#)] [[PubMed](#)]
9. Flörke, M.; Schneider, C.; McDonald, R.I. Water competition between cities and agriculture driven by climate change and urban growth. *Nat. Sustain.* **2018**, *1*, 51–58. [[CrossRef](#)]
10. Dolatyar, M.; Gray, T.S. The politics of water scarcity in the Middle East. *Environ. Politics* **2000**, *9*, 65–88.
11. Lonergan, S.; Kavanagh, B. Climate change, water resources and security in the Middle East. *Glob. Environ. Chang.* **1991**, *1*, 272–290. [[CrossRef](#)]
12. Nakoa, K.; Rahaoui, K.; Date, A.; Akbarzadeh, A. Sustainable zero liquid discharge desalination (SZLDD). *Sol. Energy* **2016**, *135*, 337–347. [[CrossRef](#)]
13. Ecim-Djuric, O.; Topisirovic, G. Energy efficiency optimization of combined ventilation systems in 700 livestock buildings. *Energy Build.* **2010**, *42*, 1165–1171. [[CrossRef](#)]
14. Norton, T.; Sun, D.-W.; Grant, J.; Fallon, R.; Dodd, V. Applications of computational fluid dynamics (CFD) in the modelling and design of ventilation systems in the agricultural industry: A review. *Bioresour. Technol.* **2007**, *98*, 2386–2414. [[CrossRef](#)]
15. Akrami, M.; Javadi, A.A.; Hassanein, M.J.; Farmani, R.; Dibaj, M.; Tabor, G.R.; Negm, A. Study of the Effects of Vent Configuration on Mono-Span Greenhouse Ventilation Using Computational Fluid Dynamics. *Sustainability* **2020**, *12*, 986. [[CrossRef](#)]
16. Mistriotis, A.; Bot, G.; Picuno, P.; Scarascia-Mugnozza, G. Analysis of the efficiency of greenhouse ventilation using computational fluid dynamics. *Agric. For. Meteorol.* **1997**, *85*, 217–228. [[CrossRef](#)]
17. Ehret, D.L.; Lau, A.; Bittman, S.; Lin, W.; Shelford, T. Automated monitoring of greenhouse crops. *Agronomie* **2001**, *21*, 403–414. [[CrossRef](#)]
18. Ferrández-Villena, M.; Ruiz-Canales, A. Advances on ICTs for water management in agriculture. *Agric. Water Manag.* **2017**, *100*, 1–3. [[CrossRef](#)]
19. Gupta, M.J.; Chandra, P. Effect of greenhouse design parameters on conservation of energy for greenhouse environmental control. *Energy* **2002**, *27*, 777–794. [[CrossRef](#)]
20. Sethi, V.P. On the selection of shape and orientation of a greenhouse: Thermal modeling and experimental validation. *Sol. Energy* **2009**, *83*, 21–38. [[CrossRef](#)]

21. Gupta, R.; Tiwari, G.; Kumar, A.; Gupta, Y. Calculation of total solar fraction for different orientation of greenhouse using 3D-shadow analysis in Auto-CAD. *Energy Build.* **2012**, *47*, 27–34. [\[CrossRef\]](#)
22. Çakır, U.; Şahin, E. Using solar greenhouses in cold climates and evaluating optimum type according to sizing, position and location: A case study. *Comput. Electron. Agric.* **2015**, *117*, 245–257. [\[CrossRef\]](#)
23. El-Maghlany, W.M.; Teamah, M.A.; Tanaka, H. Optimum design and orientation of the greenhouses for maximum capture of solar energy in North Tropical Region. *Energy Convers. Manag.* **2015**, *105*, 1096–1104. [\[CrossRef\]](#)
24. Stanciu, C.; Stanciu, D.; Dobrovicescu, A. Effect of greenhouse orientation with respect to EW axis on its required heating and cooling loads. *Energy Procedia* **2016**, *85*, 498–504. [\[CrossRef\]](#)
25. Lamrani, M.A.; Boulard, T.; Roy, J.C.; Jaffrin, A. Airflow and temperature patterns induced in a confined greenhouse. *J. Agric. Eng. Res.* **2001**, *78*, 75–88. [\[CrossRef\]](#)
26. Boulard, T.; Haxaire, R.; Lamrani, M.A.; Roy, J.C.; Jaffrin, A. Characterization and Modelling of the Air Fluxes induced by Natural Ventilation in a Greenhouse. *J. Agric. Eng. Res.* **1999**, *74*, 135–144. [\[CrossRef\]](#)
27. Sase, S.; Takakura, T.; Nara, M. Wind tunnel testing on airflow and temperature distribution of a naturally ventilated greenhouse. *ACTA Hortic.* **1984**, *148*, 329–336. [\[CrossRef\]](#)
28. Okushima, L.; Sase, S.; Nara, M. A support system for natural ventilation design of greenhouse based on computational aerodynamics. *Acta Hortic.* **1989**, *248*, 129–136. [\[CrossRef\]](#)
29. Mistrotis, A.; Arcidiacono, C.; Picuno, P.; Bot, G.P.A.; Scarascia-Mugnozza, G. Computational analysis of ventilation in greenhouses at zero- and low-wind-speeds. *Agric. For. Meteorol.* **1997**, *88*, 121–135. [\[CrossRef\]](#)
30. Papadakis, G.; Mermier, M.; Meneses, J.F.; Boulard, T. Measurement and analysis of air exchange rates in a greenhouse with continuous roof and side openings. *J. Agric. Eng. Res.* **1996**, *63*, 219–228. [\[CrossRef\]](#)
31. Montero, J.I.; Munoz, P.; Anton, A.; Iglesias, N. Computational fluid dynamic modelling of night-time energy fluxes in unheated greenhouses. *Acta Hortic.* **2005**, *691*, 403–410. [\[CrossRef\]](#)
32. Bournet, P.E.; Winiarek, V.; Chassériaux, G. Coupled energy radiation balance in a closed partitioned glass house during night using computational fluid dynamics. In Proceedings of the International Symposium on Greenhouse Cooling: Methods, Technologies and Plant Response, Almería, Spain, 24–27 April 2006.
33. Sase, S.; Reiss, E.; Both, A.; Roberts, W. A Natural Ventilation Model for Open-Roof Greenhouses. In Proceedings of the 2002 ASAE Annual Meeting, Chicago, IL, USA, 28–31 July 2002.
34. Both, A.; Reiss, E.; Mears, D.; Roberts, W. Open-roof Greenhouse Design with Heated Ebb and Flood Floor. In Proceedings of the 2001 ASAE Annual Meeting, Sacramento, CA, USA, 29 July–1 August 2001.
35. Kacira, M.; Short, T.; Stowell, R. A CFD evaluation of naturally ventilated, multi-span, sawtooth greenhouses. *Trans. ASAE* **1998**, *41*, 833. [\[CrossRef\]](#)
36. Yongxin, L.; Baoming, L.; Zhen, L.; Tao, D. CFD simulation of a naturally ventilating cooling process for a venlo greenhouse in summer. *J. China Agric. Univ.* **2004**, *9*, 44–48.
37. Baeza, E.J.; Perez-Parra, J.J.; Montero, J.I.; Bailey, B.J.; Lopez, J.C.; Gazquez, J.C. Analysis of the role of sidewall vents on buoyancy-driven natural ventilation in parral-type greenhouses with and without insect screens using computational fluid dynamics. *Biosyst. Eng.* **2009**, *104*, 86–96. [\[CrossRef\]](#)
38. Fatnassi, H.; Boulard, T.; Demrati, H.; Bouirden, L.; Sappe, G. SE—Structures and Environment: Ventilation Performance of a Large Canarian-Type Greenhouse Equipped with Insect-Proof Nets. *Biosyst. Eng.* **2002**, *82*, 97–105. [\[CrossRef\]](#)
39. Fatnassi, H.; Boulard, T.; Bouirden, L.; Sappe, G. Ventilation performances of a large canarian type greenhouse equipped with insect-proof nets. In Proceedings of the International Symposium on Design and Environmental Control of Tropical and Subtropical Greenhouses 578, 2001. [\[CrossRef\]](#)
40. Bony, S.; Lau, K.; Sud, Y. Sea surface temperature and large-scale circulation influences on tropical greenhouse effect and cloud radiative forcing. *J. Clim.* **1997**, *10*, 2055–2077. [\[CrossRef\]](#)
41. Patil, S.; Tantau, H.; Salokhe, V. Modelling of tropical greenhouse temperature by auto regressive and neural network models. *Biosyst. Eng.* **2008**, *99*, 423–431. [\[CrossRef\]](#)
42. Bournet, P.-E.; Boulard, T. Effect of ventilator configuration on the distributed climate of greenhouses: A review of experimental and CFD studies. *Comput. Electron. Agric.* **2010**, *74*, 195–217. [\[CrossRef\]](#)
43. Okushima, L.; Sase, S.; Maekawa, T.; Ikegushi, A. Airflow patterns forced by wind effect in a Venlo type greenhouse. *J. Soc. Agric. Struct. Jpn.* **1998**, *29*, 159–167.
44. Boulard, T.; Lamrani, M.A.; Roy, J.C.; Jaffrin, A.; Bouirden, L. Natural Ventilation by Thermal Effect in a one-half scale mono-span Greenhouse. *Trans. ASAE* **1998**, *41*, 773–781. [\[CrossRef\]](#)

45. Lee, I.B.; Okushima, L.; Ikegushi, A.; Sase, S.; Short, T.H. Prediction of natural ventilation of multi-span greenhouses using CFD techniques and its verification with wind tunnel test. In Proceedings of the 93rd Annual Meeting of ASAE, Paper No. 005003, Milwaukee, WI, USA, July 9–12 2000.
46. Bailey, B.J.; Robertson, A.P.; Lockwood, A.G. The influence of wind direction on greenhouse ventilation. *Acta Hortic.* **2004**, *633*, 197–202. [[CrossRef](#)]
47. Kacira, M.; Sase, S.; Ikeguchi, A.; Ishii, M.; Giacomelli, G.; Sabeh, N. Effect of vent configuration and wind speed on three-dimensional temperature distributions in a naturally ventilated multi-span greenhouse by wind tunnel experiments. *Acta Hortic.* **2008**, *801*, 393–400. [[CrossRef](#)]
48. Teitel, M.; Ziskind, G.; Liran, O.; Dubovsky, V.; Letan, R. Effect of wind direction on greenhouse ventilation rate, airflow patterns and temperature distributions. *Biosyst. Eng.* **2008**, *101*, 351–369. [[CrossRef](#)]
49. Montero, J.I.; Hunt, G.R.; Kamaruddin, R.; Anton, A.; Bailey, B.J. Effect of ventilator configuration on Wind-driven Ventilation in a Crop Protection Structure for the Tropics. *J. Agric. Eng. Res.* **2001**, *80*, 99–107. [[CrossRef](#)]
50. Kittas, C.; Draoui, B.; Boulard, T. Quantification of the ventilation of a greenhouse with a roof opening. *Agric. For. Meteorol.* **1995**, *77*, 95–111. [[CrossRef](#)]
51. Kittas, C.; Boulard, T.; Mermier, M.; Papadakis, G. Wind induced air exchange rates in a greenhouse tunnel with continuous side openings. *J. Agric. Eng. Res.* **1996**, *65*, 37–49. [[CrossRef](#)]
52. Boulard, T.; Meneses, J.F.; Mermier, M.; Papadakis, G. The mechanisms involved in the natural ventilation of greenhouses. *Agric. For. Meteorol.* **1996**, *79*, 61–77. [[CrossRef](#)]
53. Wang, S.; Deltour, J.M. Natural ventilation induced airflow patterns measured by an ultrasonic anemometer in Venlo-type greenhouse openings. *Agric. Eng. J.* **1997**, *6*, 185–196.
54. Wang, S.; Deltour, J.M. Lee-side ventilation-induced air movement in a largescale multi-span greenhouse. *J. Agric. Eng. Res.* **1999**, *74*, 103–110. [[CrossRef](#)]
55. Demrati, H.; Boulard, T.; Bekkaoui, A.; Bouirden, L. Natural ventilation and climatic performance of a large scale banana greenhouse. *J. Agric. Eng. Res.* **2001**, *80*, 261–271. [[CrossRef](#)]
56. Molina-Aiz, F.D.; Valera, D.L.; Alvarez, A.J. Measurement and simulation of climate inside Almeria-type greenhouses using computational fluid dynamics. *Agric. For. Meteorol.* **2004**, *125*, 33–51. [[CrossRef](#)]
57. Perez Parra, J.; Baeza, E.; Montero, J.I.; Bailey, B.J. Natural Ventilation of Parral Greenhouses. *Biosyst. Eng.* **2004**, *87*, 355–366. [[CrossRef](#)]
58. Katsoulas, N.; Bartzanas, T.; Boulard, T.; Mermier, M.; Kittas, C. Effect of vent openings and insect screens on greenhouse ventilation. *Biosyst. Eng.* **2006**, *93*, 427–436. [[CrossRef](#)]
59. Ould Khaoua, S.A.; Bournet, P.E.; Migeon, C.; Boulard, T.; Chasseriaux, G. Analysis of Greenhouse Ventilation Efficiency based on Computational Fluid Dynamics. *Biosyst. Eng.* **2006**, *95*, 83–98.
60. Bournet, P.E.; Khaoua, S.A.O.; Boulard, T. Numerical prediction of the effect of vents arrangements on the ventilation and energy transfers in a multispan glasshouse using a bi-band radiation model. *Biosyst. Eng.* **2007**, *98*, 224–234.
61. Bournet, P.E.; Khaoua, S.A.O.; Boulard, T.; Migeon, C.; Chasseriaux, G. Effect of roof and side opening combinations on the ventilation of a glasshouse using computer simulations. *Trans. ASABE Am. Soc. Agric. Biol. Eng.* **2007**, *50*, 201–212.
62. Teitel, M.; Liran, O.; Tanny, J.; Barak, M. Wind driven ventilation of a mono-span greenhouse with a rose crop and continuous screened side vents and its effect on flow patterns and microclimate. *Biosyst. Eng.* **2008**, *101*, 111–122. [[CrossRef](#)]
63. Fatnassi, H.; Leyronas, C.; Boulard, T.; Bardin, M.; Nicot, P. Dependence of greenhouse tunnel ventilation on wind direction and crop height. *Biosyst. Eng.* **2009**, *103*, 338–343. [[CrossRef](#)]
64. Majdoubi, H.; Boulard, T.; Fatnassi, H.; Bouirden, L. Airflow and microclimate patterns in a one-hectare Canary type greenhouse: An experimental and CFD assisted study. *Agric. For. Meteorol.* **2009**, *149*, 1050–1062. [[CrossRef](#)]
65. Baptista, F.J.; Bailey, B.J.; Randall, J.M.; Meneses, J.F. Greenhouse ventilation rate: Theory and measurement with tracer gas techniques. *J. Agric. Eng. Res.* **1999**, *72*, 363–374. [[CrossRef](#)]
66. Lee, I.B.; Sase, S.; Okushima, L.; Ikeguchi, A.; Choi, K.; Yun, J. A wind tunnel study of natural ventilation for multi-span greenhouse scale models using two-dimensional particle image velocimetry PIV. *Trans. ASAE* **2003**, *46*, 763–772.

67. Heber, A.J.; Boon, C.R.; Peugh, M.W. Air patterns in an experimental livestock building. *J. Agric. Eng. Res.* **1996**, *64*, 209–226. [\[CrossRef\]](#)
68. Boulard, T.; Papadakis, G.; Kittas, C.; Mermier, M. Air flow and associated sensible heat exchanges in a naturally ventilation greenhouse. *Agric. For. Meteorol.* **1997**, *88*, 111–119. [\[CrossRef\]](#)
69. Boulard, T.; Wang, S.; Haxaire, R. Mean and turbulent air flows and microclimatic patterns in an empty greenhouse tunnel. *Agric. For. Meteorol.* **2000**, *100*, 169–181. [\[CrossRef\]](#)
70. Bartzanas, T.; Boulard, T.; Kittas, C. Effect of Vent Arrangement on Windward Ventilation of a Tunnel Greenhouse. *Biosyst. Eng.* **2004**, *88*, 479–490. [\[CrossRef\]](#)
71. Bartzanas, T.; Kittas, C.; Sapounas, A.A.; Nikita-Martzopoulou, C. Analysis of airflow through experimental rural buildings: Sensitivity to turbulence models. *Biosyst. Eng.* **2007**, *97*, 229–239. [\[CrossRef\]](#)
72. Shilo, E.; Teitel, M.; Mahrer, Y.; Boulard, T. Air-flow patterns and heat fluxes in roof-ventilated multi-span greenhouse with insect-proof screens. *Agric. For. Meteorol.* **2004**, *122*, 3–20. [\[CrossRef\]](#)
73. Mohammadi, B.; Pironneau, O. Analysis of the k- ϵ turbulence model. In *Research in Applied Mathematics*; Wiley-Masson: Paris, France, 1994.
74. Boulard, T.; Kittas, C.; Roy, J.; Wang, S. SE—Structures and environment: Convective and ventilation transfers in greenhouses, part 2: Determination of the distributed greenhouse climate. *Biosyst. Eng.* **2002**, *83*, 129–147.
75. Ali, H.B.; Bournet, P.-E.; Danjou, V.; Morille, B.; Migeon, C. CFD simulations of the night-time condensation inside a closed glasshouse: Sensitivity analysis to outside external conditions, heating and glass properties. *Biosyst. Eng.* **2014**, *127*, 159–175.
76. Roy, J.; Boulard, T. CFD prediction of the natural ventilation in a tunnel-type greenhouse: Influence of wind direction and sensibility to turbulence models. In Proceedings of the International Conference on Sustainable Greenhouse Systems-Greensys 2004, Leuven, Belgium, September 2004. [\[CrossRef\]](#)
77. Campben, J.B.; Bot, G.P.A. Determination of Greenhouse-specific Aspects of Ventilation using Three-dimensional Computational Fluid Dynamics. *Biosyst. Eng.* **2003**, *84*, 69–77. [\[CrossRef\]](#)
78. Norton, T.; Sun, D. Computational fluid dynamics (CFD)—An effective and efficient design and analysis tool for the food industry: A review. *Trend Food Sci. Technol.* **2006**, *17*, 600–620. [\[CrossRef\]](#)
79. Rouboa, A.; Monteiro, E. Computational Fluid Dynamics analysis of greenhouse microclimates by heated underground tubes. *J. Mechan. Sci. Technol.* **2007**, *21*, 2196–2204. [\[CrossRef\]](#)
80. Nebbali, R.; Roy, J.C.; Boulard, T.; Makhlof, S. Comparison of the accuracy of different CFD turbulence models for the prediction of the climatic parameters in a tunnel greenhouse. *Acta Hortic.* **2006**, *719*, 287–294. [\[CrossRef\]](#)
81. Shyklar, A.; Arbel, A. Numerical model of the three-dimensional isothermal flow patterns and mass fluxes in a pitched-roof greenhouse. *J. Wind Eng. Ind. Aerodyn.* **2004**, *92*, 1039–1059. [\[CrossRef\]](#)
82. Ntinis, G.; Kateris, D.; Fragos, V.; Malamataris, N.; Nikita-Martzopoulou, C. Unsteady computational study of airflow characteristics around an agricultural structure model. In Proceedings of the International Symposium on Advanced Technologies and Management Towards Sustainable Greenhouse Ecosystems: Greensys 2011, 5 June 2011; pp. 185–190. [\[CrossRef\]](#)
83. Avezova, N.; Samiev, K.; Khaetov, A.; Nazarov, I.; Ergashev, Z.Z.; Samiev, M.; Suleimanov, S.I. Modeling of the unsteady temperature conditions of solar greenhouses with a short-term water heat accumulator and its experimental testing. *Appl. Sol. Energy* **2010**, *46*, 4–7. [\[CrossRef\]](#)
84. Abdel Ghany, A.M. Energy balance equation for natural ventilation of greenhouses under unsteady state conditions. *Middle East J. Sci. Res.* **2011**, *10*, 286–293.
85. Wang, S.; Boulard, T. Measurement and prediction of solar radiation distribution in full-scale greenhouse tunnel. *Agronomie* **2000**, *20*, 41–50. [\[CrossRef\]](#)
86. Fluent, A. ANSYS Fluent 12.0 user's guide. *Ansys Inc.* **2009**, 15317, 1–2498.
87. Lee, I.B.; Short, T.H. Two-dimensional numerical simulation of natural ventilation in a multi-span greenhouse. *Trans. ASAE* **2000**, *43*, 745–753. [\[CrossRef\]](#)
88. Boulard, T.; Feuilloley, G.; Kittas, C. Natural ventilation performance of six greenhouse and tunnel type. *J. Agric. Eng. Res.* **1997**, *67*, 249–266. [\[CrossRef\]](#)
89. Boulard, T.; Wang, S. Experimental and numerical studies on the heterogeneity of crop transpiration in a plastic tunnel. *Comput. Electron. Agric.* **2002**, *173*, 190–234. [\[CrossRef\]](#)
90. Campiotti, C.A.; Morosinotto, G.; Puglisi, G.; Schettini, E.; Vox, G. Performance evaluation of a solar cooling plant applied for greenhouse thermal control. *Agric. Agric. Sci. Procedia* **2016**, *8*, 664–669. [\[CrossRef\]](#)

91. Picha, D. Horticultural crop quality characteristics important in international trade. In Proceedings of the IV International Conference on Managing Quality in Chains-The Integrated View on Fruits and Vegetables Quality, 7 August 2006; pp. 423–426. [\[CrossRef\]](#)
92. Willits, D. Cooling fan-ventilated greenhouses: A modelling study. *Biosyst. Eng.* **2003**, *84*, 315–329. [\[CrossRef\]](#)
93. Boulard, T.; Baille, A. Modelling of air exchange rate in a greenhouse equipped with continuous roof vents. *J. Agric. Eng. Res.* **1995**, *61*, 38–48. [\[CrossRef\]](#)
94. Bartzanas, T.; Kittas, C. Optimisation of greenhouses ventilation performance with computational fluid dynamics. In Proceedings of the 2nd Southeastern Europe Fluent Users Group Meeting, Bucharest Romania, 31 October–2 November 2001.
95. Lee, I.B.; Short, T.H. Computational fluid dynamic study for structural design of naturally ventilated multi-span greenhouses. In Proceedings of the 92nd Annual International Meeting of ASAE, Toronto, ON, Canada, 18–21 July 1999.
96. Kittas, C.; Boulard, T.; Papadakis, G. Natural ventilation of a greenhouse with ridge and side openings: Sensitivity to temperature and wind effects. *Trans. ASAE* **1997**, *40*, 415–425. [\[CrossRef\]](#)
97. Bartzanas, T.; Boulard, T.; Kittas, C. Numerical simulation of the airflow and temperature distribution in a tunnel greenhouse equipped with insect-proof screen in the openings. *Comput. Electron. Agric.* **2002**, *34*, 207–221. [\[CrossRef\]](#)
98. Kacira, M.; Sase, S.; Okushima, L. Effects of side vents and span numbers on wind-induced natural ventilation of a gothic multi-span greenhouse. *Jpn. Agric. Res. Q.* **2004**, *38*, 227–233. [\[CrossRef\]](#)
99. Molina-Aiz, F.D.; Valera, D.L. Optimization of Almeria-type greenhouse vent configuration by evaluating ventilation efficiency based on computational fluid dynamics. *Acta Hortic.* **2011**, *893*, 669–677. [\[CrossRef\]](#)
100. Boulard, T.; Fatnassi, H. Greenhouse aeration and climate optimization based on CFD studies. *Plasticulture* **2005**, *124*, 38–57.
101. Sanford, S. Reducing greenhouse energy consumption—An overview. *Energy* **2011**, 3907. Available online: https://fyi.extension.wisc.edu/energy/files/2018/07/reducing_greenhouse_energy_consumption_-_an_overview.pdf (accessed on 20 March 2020).
102. Zhang, G.; Ding, X.; Li, T.; Pu, W.; Lou, W.; Hou, J. Dynamic energy balance model of a glass greenhouse: An experimental validation and solar energy analysis. *Energy* **2020**, *198*, 117281. [\[CrossRef\]](#)
103. Short, T.H.; Lee, I.B. Temperature and airflow predictions for multi-span naturally ventilated greenhouse. *Acta Hortic.* **2002**, *578*, 141–152. [\[CrossRef\]](#)
104. Baeza, E.J.; Perez-Parra, J.; Montero, J.I. Effect of ventilator size on natural ventilation in parral greenhouse by means of CFD simulations. *Acta Hortic.* **2004**, *691*, 465–472. [\[CrossRef\]](#)
105. Ortiz, D.M.; Acuna, J.F. Natural numerical simulation of ventilation in a Colombian greenhouse. *Pasticulture* **2005**, *124*, 58–71.
106. Arbel, A.; Yekutieli, O.; Barak, M. Performance of a fog system for cooling greenhouses. *J. Agric. Eng. Res.* **1999**, *72*, 129–136.
107. Baille, A.; Kittas, C.; Katsoulas, N. Influence of whitening on greenhouse and crop energy partitioning. *Agric. For. Meteorol.* **2001**, *107*, 293–306. [\[CrossRef\]](#)
108. Katsoulas, N.; Baille, A.; Kittas, C. Effect of misting on transpiration and conductances of a greenhouse rose canopy. *Agric. For. Meteorol.* **2001**, *106*, 233–247. [\[CrossRef\]](#)
109. Kim, K.; Yoon, J.; Kwon, H.; Han, J.; Son, J.; Nam, S.; Giacomelli, G.; Lee, I. 3-D CFD analysis of relative humidity distribution in greenhouse with a fog cooling system and refrigerative dehumidifiers. *Biosyst. Eng.* **2008**, *100*, 245–255. [\[CrossRef\]](#)
110. Piscia, D.; Munoz, P.; Panades, C.; Montero, J.I. A method of coupling CFD and energy balance simulations to study humidity control in unheated greenhouses. *Comput. Electron. Agric.* **2015**, *115*, 129–141. [\[CrossRef\]](#)
111. Percy, R.W.; Schulze, E.; Zimmermann, R. Measurement of transpiration and leaf conductance. In *Plant Physiological Ecology*; Springer: Dordrecht, The Netherlands, 2000.
112. Boulard, T.; Mermier, M.; Fargues, J.; Smits, N.; Rougier, M. Tomato leaf boundary layer climate: Implication for microbiological control of whiteflies in greenhouse. *Agric. For. Meteorol.* **2002**, *110*, 159–176. [\[CrossRef\]](#)
113. Fatnassi, H.; Boulard, T.; Poncet, C.; Chave, M. Optimisation of greenhouse insect screening with computational fluid dynamics. *Biosyst. Eng.* **2006**, *93*, 301–312. [\[CrossRef\]](#)
114. Fatnassi, H.; Boulard, T.; Lagier, J. Simple Indirect Estimation of Ventilation and Crop Transpiration Rates in a Greenhouse. *Biosyst. Eng.* **2004**, *88*, 467–478. [\[CrossRef\]](#)

115. Hagishima, A.; Narita, K.; Tanimoto, J. Field experiment on transpiration from isolated urban plants. *Hydrol. Process.* **2007**, *21*, 1217–1222. [[CrossRef](#)]
116. Kichah, A.; Bournet, P.E.; Migeon, C.; Boulard, T. Measurement and CFD simulation of microclimate characteristics and transpiration of an Impatiens pot plant crop in a greenhouse. *Biosyst. Eng.* **2012**, *112*, 22–34. [[CrossRef](#)]
117. Iga, J.L.; Iga, J.L.; Iga, C.L.; Flores, R.A. Effect of air density variations on greenhouse temperature model. *Math. Comput. Model.* **2008**, *47*, 855–867.
118. Dayioğlu, M.A.; Silileli, H.H. Performance analysis of a greenhouse fan-pad cooling system: Gradients of horizontal temperature and relative humidity. *Tarım Bilim. Derg.* **2015**, *21*, 132–143. [[CrossRef](#)]
119. Sablani, S.; Goosen, M.; Paton, C.; Shayya, W.; Al-Hinai, H. Simulation of fresh water production using a humidification-dehumidification seawater greenhouse. *Desalination* **2003**, *159*, 283–288. [[CrossRef](#)]
120. Goosen, M.; Sablani, S.; Paton, C.; Perret, J.; Al-Nuaimi, A.; Haffar, I.; Al-Hinai, H.; Shayya, W. Solar energy desalination for arid coastal regions: Development of a humidification–dehumidification seawater greenhouse. *Sol. Energy* **2003**, *75*, 413–419. [[CrossRef](#)]
121. Davies, P. A solar cooling system for greenhouse food production in hot climates. *Sol. Energy* **2005**, *79*, 661–668. [[CrossRef](#)]
122. Davies, P.; Paton, C. The Seawater Greenhouse: Background, theory and current status. *Int. J. Low Carbon Technol.* **2006**, *1*, 183–190. [[CrossRef](#)]
123. Dawoud, B.; Zurigat, Y.; Klitzing, B.; Aldoss, T.; Theodoridis, G. On the possible techniques to cool the condenser of seawater greenhouses. *Desalination* **2006**, *195*, 119–140. [[CrossRef](#)]
124. Kabeel, A.E.; El-Said, E.M.S. Water production for irrigation and drinking needs in remote arid communities using closed-system greenhouse: A review. *Eng. Sci. Technol. Int. J.* **2015**, *18*, 294–301. [[CrossRef](#)]
125. Bourouni, K.; Chaibi, M.T.; Al-Tae, A. Water desalination by humidification and dehumidification of air, seawater greenhouse process. In *Solar energy conservation and photoenergy systems. Encyclopedia of Life Support Systems (EOLSS)*; UNESCO: Paris, France, 2011. Available online: <http://www.eolss.net/Sample-Chapters/C08/E6-106-47.pdf> (accessed on 20 March 2020).
126. Mahmoudi, H.; Spahis, N.; Abdul-Wahab, S.A.; Sablani, S.S.; Goosen, M.F. Improving the performance of a Seawater Greenhouse desalination system by assessment of simulation models for different condensers. *Renew. Sustain. Energy Rev.* **2010**, *14*, 2182–2188. [[CrossRef](#)]
127. Salehi, G.; Ahmadpour, M.; Khoshnazar, H. Modeling of the seawater greenhouse systems. In Proceedings of the World Renewable Energy Congress-Sweden, Linköping, Sweden, 8–13 May 2011.
128. Kabeel, A.; Almagar, A.M. Seawater greenhouse in desalination and economics. In Proceedings of the Seventeenth International Water Technology Conference, IWTC17, Istanbul, Turkey, 5–7 November 2013.
129. Al-Ismaili, A.M.; Jayasuriya, H. Seawater greenhouse in Oman: A sustainable technique for freshwater conservation and production. *Renew. Sustain. Energy Rev.* **2016**, *54*, 653–664. [[CrossRef](#)]
130. Katsoulas, N.; Savvas, D.; Tsirogiannis, I.; Merkouris, O.; Kittas, C. Response of an eggplant crop grown under Mediterranean summer conditions to greenhouse fog cooling. *Sci. Hortic.* **2009**, *123*, 90–98. [[CrossRef](#)]
131. Lu, N.; Nukaya, T.; Kamimura, T.; Zhang, D.; Kurimoto, I.; Takagaki, M.; Maruo, T.; Kozai, T.; Yamori, W. Control of vapor pressure deficit (VPD) in greenhouse enhanced tomato growth and productivity during the winter season. *Sci. Hortic.* **2015**, *197*, 17–23. [[CrossRef](#)]
132. Cohen, Y.; Stanhill, G.; Fuchs, M. An experimental comparison of evaporative cooling in a naturally ventilated glasshouse due to wetting the outer roof and inner crop soil surfaces. *Agric. Meteorol.* **1983**, *28*, 239–251. [[CrossRef](#)]
133. Al-Helal, I.M.; Abdel-Ghany, A.M. Responses of plastic shading nets to global and diffuse PAR transfer: Optical properties and evaluation. *NJAS Wagening. J. Life Sci.* **2010**, *57*, 125–132. [[CrossRef](#)]
134. Chaibi, M.T. Analysis by simulation of a solar still integrated in a greenhouse roof. *Desalination* **2000**, *128*, 123–138. [[CrossRef](#)]
135. El-Awady, M.; El-Ghetany, H.; Latif, M.A. Experimental investigation of an integrated solar green house for water desalination, plantation and wastewater treatment in remote arid Egyptian communities. *Energy Procedia* **2014**, *50*, 520–527. [[CrossRef](#)]
136. Chaibi, M.T.; Jilar, T. Effects of a Solar Desalination Module integrated in a Greenhouse Roof on Light Transmission and Crop Growth. *Biosyst. Eng.* **2005**, *90*, 319–330. [[CrossRef](#)]

137. Mari, E.G.; Colomer, R.P.G.; Blaise-Ombrecht, C.A. Performance analysis of a solar still integrated in a greenhouse. *Desalination* **2007**, *203*, 435–443. [[CrossRef](#)]
138. Yildiz, A.; Ozgener, O.; Ozgener, L. Exergetic performance assessment of solar photovoltaic cell (PV) assisted earth to air heat exchanger (EAHE) system for solar greenhouse cooling. *Energy Build.* **2011**, *43*, 3154–3160. [[CrossRef](#)]
139. Sethi, V.; Sharma, S. Experimental and economic study of a greenhouse thermal control system using aquifer water. *Energy Convers. Manag.* **2007**, *48*, 306–319. [[CrossRef](#)]
140. Entezari, A.; Wang, R.; Zhao, S.; Mahdinia, E.; Wang, J.; Tu, Y.; Huang, D. Sustainable agriculture for water-stressed regions by air-water-energy management. *Energy* **2019**, *181*, 1121–1128. [[CrossRef](#)]



© 2020 by the authors. Licensee MDPI, Basel, Switzerland. This article is an open access article distributed under the terms and conditions of the Creative Commons Attribution (CC BY) license (<http://creativecommons.org/licenses/by/4.0/>).